Phase Change Material Mixed with Chloride Salt Graphite Foam Infiltration for Latent Heat Storage Applications at Higher Temperatures and Pressures

Mostafa Esmaeili Shayan*[1], Gholamhassan Najafi[2], Giulio Lorenzini[3]

[1] *Department of Biosystem Engineering, Tarbiat Modares University, Tehran, Iran, E.mostafa@modares.ac.ir*

[2] *Department of Biosystem Engineering, Tarbiat Modares University, Tehran, Iran, g.najafi@modares.ac.ir*

[3] *Department of Engineering and Architecture, University of Parma, Parco Area Delle Scienze, Parma, Italy, giulio.lorenzini@unipr.it*

Abstract

In the address layer of energy systems, the infiltration of phase-change material (PCM) into composite metals can be used. In this study, infiltration technology was developed with simultaneous pressure and vacuum in graphite foam. The vacuum pump was used to create porosity during the melting and infiltration process in the composition of PCM pellets. Easy construction, stainless steel, and PCM's corrosion-resistant function deliver a Cost-efficient and simple process development. The goal of this analysis is to examine the properties of PCM using a mixture of materials such as salts and chloride salts with graphite foam. High energy storage density Chloride-based PCM was used at 355 degrees Celsius. The energy dispersive spectroscopy and Scanning electron microscopy analysis were used to assess the successful existence of the phase of infiltration to test the PCM composite and material compounds. A laser thermal flash conductivity meter was used to evaluate the infiltrated sample thermal conductivity. An infiltration performance of more than 92% of the porosity usable has been reached. The Sample thermal conductivity is proven to be more robust Factor more than 45 times pure chloride PCM. Low-cost infiltration demonstrated effectiveness and Infiltrated PCM repeatability may be a milestone for the third generation of supercritical carbon dioxide energy cycle applications in concentrating solar power plants.

Keywords: Infiltration; Phase-Change Material (PCM); Graphite Foam; Thermal Conductivity; Energy.

Nomenclature

Preferred name	**Symbols**	**Unit**	***Subscript***	
Volume	V	m^3	a	After infiltration
Efficiency	η	%	b	Before infiltration
Energy storage density loss	L	%	ini	Initial
Infiltrated	inf	unitless	sf	Soaking fluid
Normal Density	ρ	$kg \cdot m^{-3}$	***Acronyms***	
Porosity	Φ	pu	*TES*	Thermal Energy Storage
Pressure	p	Pascal [Pa]	*CSP*	Concentrated Solar Power
Specific heat capacity	Cp	$J \cdot kg^{-1} \cdot K^{-1}$	*EDS*	Energy Dispersive Spectroscopy
Thermal conductivity	k	$W \cdot m^{-1} \cdot K^{-1}$	*LHTES*	Latent Heat Thermal Energy Storage
Thermal diffusivity	α	$m^2 \cdot s^{-1}$	*PCM*	Phase Change Material
Weight changes	ΔW	gr	*SEM*	Scanning Electron Microscope

1. Introduction

The transient existence of solar energy and demand mismatch demands that thermal energy storage (TES) become an essential component of solar power production. In an attempt to lessen solar energy costs, for next generation CSP systems in particular, Higher storage of electricity ability is desirable at higher storage temperatures. A characteristic of potential CSP plants would be at high temps, higher processing Storage density. Apart from energy storage capacity, Storage rates are the important point for designing supercritical power cycles for content storage [1,2]. Latent thermal energy storage (LHTES) utilizing salts will have a more power storage volume, almost continuous charging of temperature, and transfers of energy from the discharge, non-toxic media, at an economical price relative to responsive TES methods [3,4]. Given the benefits, LHTES systems have substantial limitations for large-scale high-temperature applications [5]. Researchers found that in PCM materials, specifically in PCM materials with alkaline salt bases, corrosion and conductivity are key [6]. TES systems appropriate to CSP plants need more generous primary storage space at acceptable storage/deployment rates [7]. The heat distribution improvements used to cope with low thermal conductivity involve finned tubing, embedded heat pipes, and foam systems. The last of these methods of change is the focus of ongoing operations Chlorides are extremely fragile regardless of the temperature of nitrate may be used as possible PCMs at extreme temperatures. Chlorides, particularly in high-temperature conditions, can be very corrosive[8,9]. Therefore, traditional metallic improvements to heat transmission may not suitable for these circumstances.

Due to high capacity and specifications the PCM content is no longer required for a significant number of thermal graphite foams [10]. Graphite products can be appealing in thermal energy storage applications with neutral corrosion characteristics[11]. some materials are used to improve PCM thermal conductivity. this material contributes to certain compromises required for overall thermal energy density as foam media do not participate as a PCM. As stated later, such compromises are warranted because foams will significantly increase the entire storage device's thermal conductivity. Due to some of the graphite foam system's select properties, several researchers have used them to enhance thermal conductivity. A new review and assessment of a variety of improved PCM's thermal conductivity has been published. This research was used in low-temperature applications with the use of graphite foams. Heat transfer rise in phase shift Embedded Substances Pore Materials and polymers was examined by Hajjar et al. [12]. Karthik et al. used thermal conductivity graphite foam to enhance the pure paraffin wax. Paraffin wax – graphite foam hybrid was more thermally conductive than straight paraffin wax, up to 570 times [13]. Lan et al. also examined high density, different temperatures, and pressures, graphite foam infiltrated with paraffin. Compared with paraffin, it has been demonstrated that the composite's thermal conductivity can be improved by 768 times [14]. Yin et al. Tested the thermal energy conservation graphite/paraffin hybrid numerically and experimentally. There have been studies of substantial increases in inefficient thermal conductivity [15]. El Idi & Karkri has researched

PCM for low-temperature applications as a nominee composite. Thermal conductivity was 11 times greater at the solid phase and 16 times more vital at the liquid phase than pure paraffin (PCM) [16]. Badenhorst Tested KCl2 mixtures of Extended industrial graphite and natural Carbon active foam for Solar thermal storage and observed substantial thermal conductivity improvements [17]. Karthik et al. contrasted clear submergence and media vacuum infiltration in foams and illustrated improved paraffin wax infiltration [13]. Mitran et al. also researched composite material and high-temperature eutectic KNO3/NaNO3 device. Uniaxial and isostatic compression is used for the preparation of composites [18]. Cheneler & Kennedy Compared paraffin wax infiltration with and without vacuum in the foam. They demonstrated dramatically higher efficiencies in vacuum-assisted infiltration[19]. Al-Jethelah et al. also researched cyclohexane-infiltrated graphite foam as a PCM, with significant increases in PCM heat conductivity [20]. Numerical calculations were also performed to predict thermal conductivities that were compatible with the test results present. Quite little study has been conductivity at high temperatures for products for phase change of graphite foam. Jana et al. found to demonstrate composites for solar thermal applications for shift in products at high temperature. In a further review, thermal conductivity research of phase change products at temperatures above 300 °C has explored classifying and innovation in thermal energy storage (TES) systems and special reservoirs [21,22]. The materials used in energy systems must have desirable thermal conductivity properties. Opolot et al has been studying the usage of graphite foam in TES in CSP plants. The research has shown that the correct use of materials will significantly minimize the amount of PCM lines used in thermal tanks [1]. Canseco et al. carried out detailed sodium nitrate research in PCM with graphite foam. The thermal information is required for Pipes used in heat tanks and PCM heat exchangers require thermal analysis. Changes in the thermal resistance of some heat exchanger surfaces improved the performance of the system [23]. Singh et al. Examined MgCl2 infiltrated PCM foam graphite. Composite thermal output and energy consumption as LHTES systems have been shown to be dramatically improved [24]. This advantage has permitted Rajak et al. to use the melting process for injecting sodium sulfate (Na_2SO_4) into SiC ceramic foam [25]. The heat efficiency of energy storage tanks is directly related to thermal composite conductivity (TCT) and 6W/m.K was stated to have the energy contained at approximately 161 kJ/kg in the studied composite. They demonstrated that its properties are preserved if high temperatures are used in the composite graphite foam process. Jiang et al. researched on MgCl2-infiltrated graphite foam as PCM for strong thermal conductivity. The penetrated composite has been tested for LHTES applications at elevated temperatures. They used a two-stage infiltration technique, where the foam is stored in a lower part of the vacuum. Graphite foam with a back pressure is applied to create the final phase of infiltration into the PCM and 714 °C was the PCM melting point. infiltration has been shown to have a marginal impact On PCM's freezing/melting point. Two forms of graphite foam were tested, one High-density and low density PCM. In relation to pure PCM, the thermal conductivity of MgCl2 is increased to 200 times by changing the structure and utilizing highest graphite foam in PCM composites. In addition, the use of low density graphite foam has increased thermal conductivity up to

30 times within the composite material. This effect can be supports the storage rates and resolves low PCM thermal conductivity, particularly under extreme temperatures. The infiltration efficiency of HD foams is recorded at 70% and LD foams at 71% [26]. Lin et al analysis a prototype of a thermal storage tank with graphite poles and composite construction and examination of the salt. At more than 700 degrees the thermal loading and unloading period was conducted. The findings of the study revealed that there is a strong connection between experimental and computational research. This research has also shown that MgCl2 graphite foam hybrid can be an appropriate material to store latent heat systems at high-temperature because it has a sufficient heat storage capacity, a limited range of operation and heat transfer enhancements [27,28].

A review of the resource data was conducted with limited research on PCM foam graphite composites at high temperatures. Corrosion, thermal conductivity, heat Storage and the cost and industrial production of the composite material are the main concerns[29,30]. In previous studies, the implemented infiltration processes are performed in multiple chambers, which complicate device design and application[31]. Given the demonstrated efficacy of graphite foam PCM infiltration in high-temperature applications, difficulty in process and the subsequent The expensive and complex manufacturing method of layers and substrates and the final processing costs restrict the usage of TES composites.

Our research has developed a system for identifying graphite pores and injecting PCM into these pores in a vacuum and pressurized condition. Compared to other methods, the whole process of infiltration of PCM material is done in one vacuum chamber at high pressure and there is no moving component involved. In this study, Samples of graphite foam/PCM prepared by SEM/EDS microanalysis have been investigated for the effectiveness of the infiltration into porous materials. Thermal conductivity analyzes, infiltration effectiveness tests und power storage density was used to classify infiltrated samples. The durability of PCM thermal infiltration was tested at melting and freezing temperatures in order to verify the validity analysis of the infiltration. Because of the simplification of infiltration and power and the likelihood of utilizing stainless to simplify the setup of a single-chamber infiltration device, the completed costs of composited preparation are anticipated to fall well short of other typical methods, which are highly needed for different systems. The final consequence of this method is the mass production of cheap PCM composite samples for LHTES applications with high temperature, required for s-CO_2 power cycles Gen3 of CSP. The aim of this research is to develop graphite/PCM foam composites for high temperature applications and an improved hybrid vacuum and pressure assisted infiltration process to demonstrate that it is an effective way of penetrating PCM into the pores of graphite foam.

2. Materials and Methods

2.1. Graphite foam

Graphite foam made of CFOAM (35 HTC) in cubes has been used in our work. Table 1 reports the properties, units and ranges of graphite foam variables. Dependent on the SEM dimensions illustrated in section 4, discussion of the results, the graphite foam pores size is about 500–600 μm, roughly half size of the vendor. The graphite foam is used in a suitable shape and size and The heat transfer of the system is not isotropic. In this research, sample architectures for infiltration have been cylindricalized from the cube (~50 mm height and ~25 mm diameter) to fit into the application-designed filtration apparatus. The graphite foam was sliced similar to water jet operation that the poozr The thermal conductivity direction is in the path of the cylinders' main axis. The determinable thermal conductivity exists in the radial direction at higher temperatures.

Table 1. properties, units and ranges of graphite foam variables[13]**.**

Characteristic	Range	Unit
Normal Density	400–500	$\frac{kg}{m^3}$
Thermal conductivity	140–180	$\frac{W}{m \cdot K}$
Percentage of holes	>70	%
Mean cavity size	1,200	μm

2.2. Phase Change Material (PCM)

Dynalene has over 40 products that can be easily mixed with water to improve heat exchanger efficiency and low chiller thermal and thermoelectric output. In this analysis the Dynalene MS-XTT hybrid (alkali and alkaline chloride salts) was used to create a mixture of chloride salt molten. The melting point of this salt is 355 °C, the normal density is 1500 kg. m^{-3}, and the energy density is 200 $kJ.kg^{-1}.K^{-1}$. The normal material density is recorded in the liquid state and at 700 °C. The high energetic density, and thermal stability render this salt a reasonable solution for high-temperature LHTES systems. PCM is penetrated into the graphite foam through compressed capsules of around 10 mm diameter. Also, during the infiltration technique's vacuum process, PCM has been subjected to sufficient environment vacuum conditions for enhanced air separation from its foam.

2.3 The Procedure and Infiltration

Dynalene develops mixed chloride and alkaline salts for the instance of PCM for corrosion, chloride in graphite foam matrix for latent thermal storage. Chloride salt is not the major melting temperature point used for this infiltration, the emphasis is on infiltration and chloride methods that may be used successfully at far higher temperatures. The Chloride PCM's unusual corrosion tolerance offers stainless steel instead of super alloys for certain hot conditions and corrosive activity environments. The probability of utilizing stainless steel extensively decreases the finished expense of the installation[23].

A designed prototype hybrid vacuum and pressure-assisted infiltration system may be carried out at minor or major scales. The installation consists of one chamber without any shifting parts, which substantially improves current installations. In the air removal phase, the PCM utilized became pelletized to have ample porosity while preserving the PCM until it melts. The usage of granulated PCM removes the need to transfer the hot fluid PCM after melting. These and further advances in PCM management remove the need for separated Hot liquid PCM transmission and PCM melting chamber and associated control facilities. Effective vacuum, high pressures and system temperature were used to manage its PCM's infiltration. Cylindrical sections were infiltrated using the methods designed for the produced unit. the infiltration system is operated for the initial stage of the phase under a high vacuum. In the second stage, the infiltration is completed using pressure, the system keeps the temperature and pressure constant while the PCM penetrates the removed foam. The basic one-room design without moving parts that only external temperature and pressure regulation were required can be seen schematically in Fig. 1.

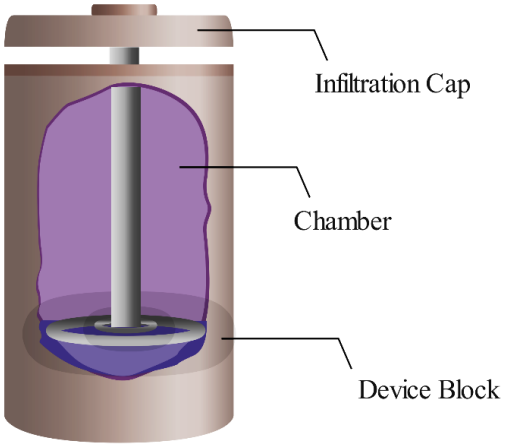

Figure 1. 2D Model of infiltration device.

In the form of PCM capsules, the graphite foam infiltrates the system more than the required pores, and when the capsule melts, the infiltration phase is complete. Events like vacuuming and air pressure nitrogen bottle was conducted up to 1.100 kPa when the screened in oven infiltration machine became just above PCM melting point. The vacuum and nitrogen-connected infiltration system in the oven could be seen in Fig. 2. Air was removed and pumped by a pressure vacuum pump from the system, and the voids were then loaded with PCM since the machine was heated over 360 Celsius degrees in a vacuum. If the PCM became supposed to melt entirely, it was compressed into a foam void using nitrogen to infiltrate PCM. Periodic vacuum purge and continuous nitrogen pressure cycle ended the infiltration step at the final stage of the equipment temperature of 500 °C.

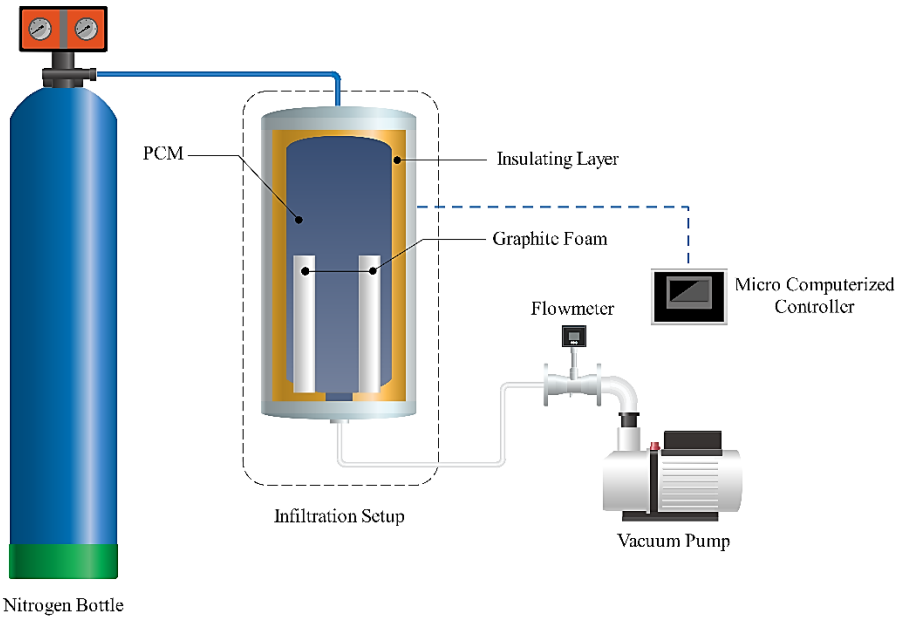

Figure 2. System schematic of vacuum and nitrogen connected infiltration.

During the cooling and infiltration phase of the composite material, a drill saw system is used to remove the excess graphite foam cylinders. The amount of cavities filled by graphite foam in vacuum environment by PCM will be higher. Compared to the total accessible volume in a graphite foam sample, this explains the efficiency of infiltration as the sample volume filled with PCM. Two samples were prepared to employ numerous methods for calculating infiltration performance quantity. Sample one was extracted in the infiltration method as an industries solidification extraction after PCM.

This calculation was made for the tests with the same original measurements and volume before and after infiltration. The specification of the correct surface tension inert soaking fluid is highly crucial for the precision of this Because of its specific outcome on the soaking process and subsequent quality of the steps on the physical size and surface tension and viscosity. Calculations Alkyl HF-LO dynalite. The hydrocarbon mixture density is not reactive. when all cavities are filled with PCM, the infiltration function is completed. The infiltration efficiency is equivalent to the final sample's weight ratio to the nominal sample weight. In other terms, the ratio of infiltrations (filling with PCM) with the highest potential PCM (having to fill all pores) is that of infiltrated graphite foam voids. The volumetric efficiency of infiltration is directly related to the volume of the PCM filled cavity. Equation 1 shows that the permeation efficiency is equal to the ratio of the volume filled with PCM to the total volume of the cavity before the infiltration process.

$$\eta_{Inf} = \frac{V_a}{V_b} \times 100 \qquad (1)$$

Where, V_b is the total sample pore before infiltration, which is described in Equation 2., and V_a is the total sample pore after infiltration. The initial before infiltration sample pore volume based on weight

is determined differences calculated before and after the soaking procedure for the pre-infiltration test, as mentioned above.

$$V_a = \frac{\Delta W_{ini} - \Delta W_{inf}}{\rho_{sf}} \quad (2)$$

$$V_b = \frac{\Delta W_{ini}}{\rho_{sf}} \quad (3)$$

Where, ΔW_{ini} is the weight change for an original non-infiltered sample following soaking and ρ_{sf} is the density of the watery fluid. Two forms of infiltrated samples were measured for η_{Inf} .Complete pores filled are measured in the original and final infiltration samples after the soaking method and ΔW_{inf} is the weight difference during the soaking step for the infiltrated sample. the main experimental errors in infiltration performance calculation are:

- Cleaning and separation of the sample from the PCM will cause PCM infiltration efficiency errors when weighed.
- Unfinished sample cleaning after removal contributing to overestimation of the weight of the sample.
- Incomplete method of soaking.
- A processing error is caused by evaporation and weight loss of material in which the sample has been soaked.

2.3.1 Thermal conductivity of samples

Different methods for measuring thermal conductivity are used. In this study Nano flash is used for the thermal conductivity of the samples. The Netzsch unit determined according to temperature and holds the penetrating foam in a clamp mounted to a thin wafer of ($\sim 12.7mm \times 12.7mm \times 4\frac{1}{4}mm$. The Netzsch furnace manages the temperature of the original sample. The rear surface temperature variations were determined using an infrared detector (IR). The thermal conductivity of the sample is calculated by the period for thermal diffusion. In the direction of a broader magnitude, thermal conductivity calculation was carried out to temperatures only below the 355 °C. During the thermal process, the sample is heated to 200°C. Then continue the heating process with a gradient of 4°C to 400°C and keep it constant at 400°C for 30 minutes. After this step, the sample returns to the base temperature and kept at this temperature for 30 minutes. This process is repeated 3 times. The sample is then cooled to room temperature and equilibrated. The weight of the sample is recorded and measured during the thermal analysis. The weight loss due to the removal of the infiltrated PCM during the thermal analysis proves the imbalance of the infiltration cycle.

2.3.2 Compositional and microstructural analytics

The sample was used for scanning electron microscopes (SEM), and the pressure of the SEM chamber was sustained for 0.005 Pa. The prepared sample was a wafer with a diameter of 2.54 cm and a height of 0.635 cm (Complies with standard inch data: 1 in and 1⁄4 in). SEM, especially TESCAN VEGA SBU, is a multi-functional tool for studying the composition of carbon foam, used to map the surface structure and morphology of materials with a resolution of a few nanometers; it also provides qualitative (BSE) and Quantitative (EDX, lateral resolution of approximately 1 μm) chemical information. Energy Dispersive Spectroscopy (EDS) is also used to track infiltration, and local chemical assessment is performed by evaluating the X-ray spectrum released from a sample flooded by a focused electron beam. SEM-image and live elemental composition study was integrated into the tungsten filament electron (TFE) stream.

3. Results and Discussions

Fig. 3. displays the graphite foam examined with optical photographic measurements pre and post infiltration. The optical photographs are obtained from cross-section samples. The infiltration method was shown fully by the filled pores with white salt, which effectively filled all pores with graphite foam.

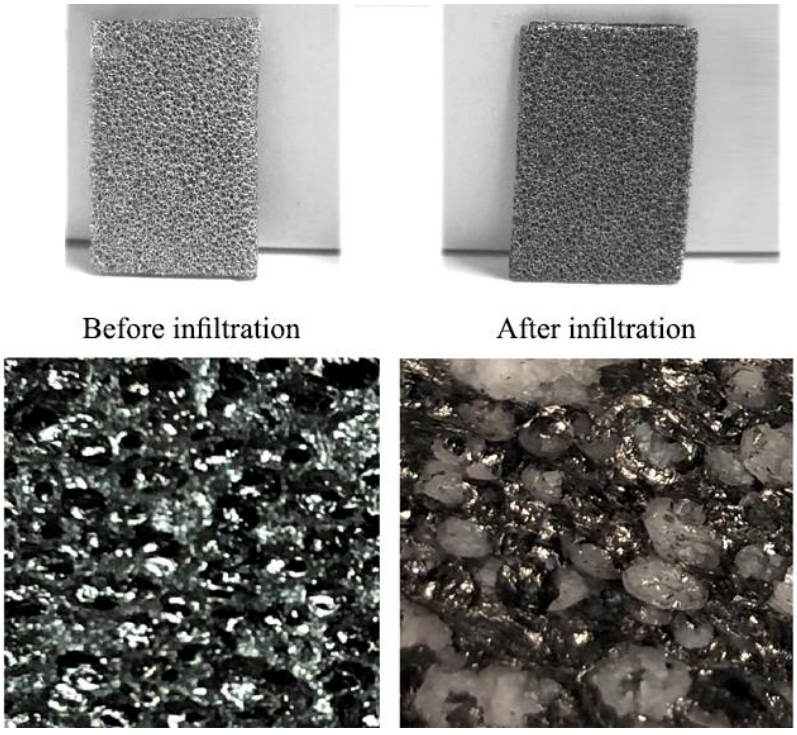

Figure 3. Optical photographic images of graphite foam pre and post infiltration.

SEM visual photos are seen in Fig.4a before infiltration along with estimated pore sizes. The diameters of the pore assessed ranged from 180 to 984 μm.

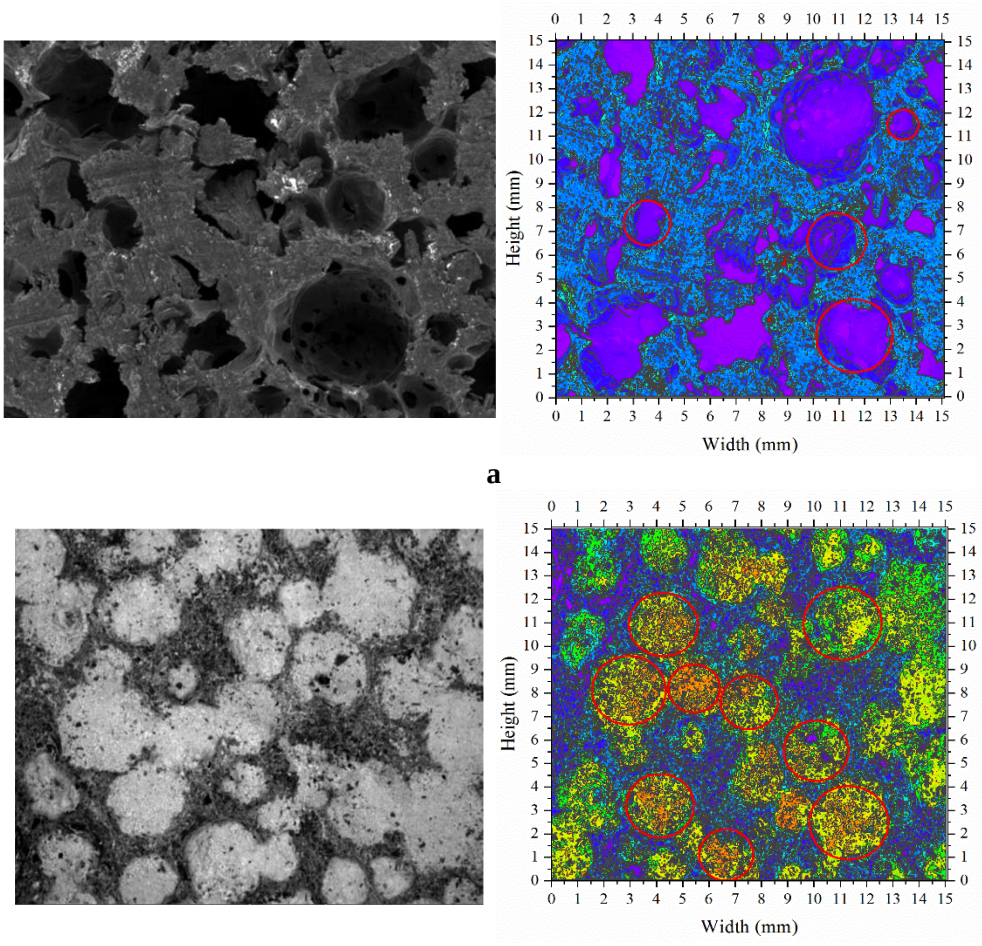

Figure 4. Optical SEM picture. a: Pre infiltration b: Post infiltration.

At a magnification of Figure 4a and Figure 4b, the difference between the infiltrated samples can be seen. Sample dimensions are shown on the 15 mm axis to understand sample pore dimensions. In the sample of Figure 4a, the number of cavities with large dimensions can be seen, while in the infiltrated sample, the cavities are filled, and the samples are denser. The EDS compositional picture and the graphite foam chart are shown before and after infiltration. The elemental carbon map is shown in blue. This is a better guide for contrast during filtration. SEM scans of the sample, as seen in Figure 4b Post infiltration. The diameters of the infiltrated pore estimated were between 395 and 844 μm. The expansion and scale of the voids are seen throughout Figure 5 in the foam structure, and the porosity framework is presented. The infiltration is complete mainly as almost all pores are loaded with PCM, also in the central part of the sample. Made images check that the infiltration method and the vacuum and pressure method built in this study are efficient ways of having PCM penetrated theoretical pores (In the range of 100 micrometers to 200 micrometers).

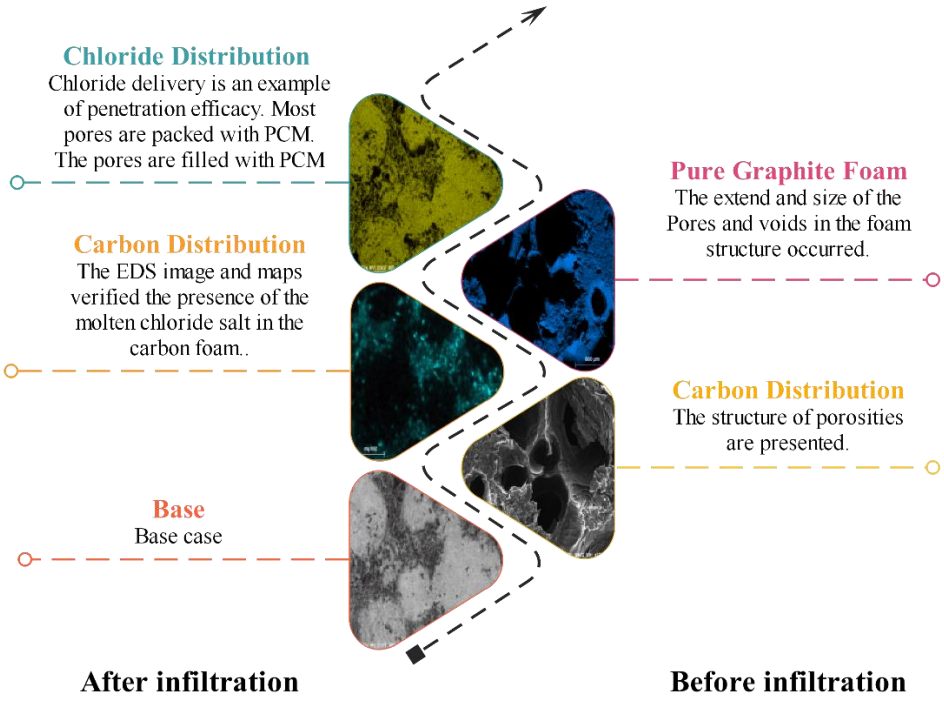

Figure 5. PCM/graphite foam composite EDS.

Figure 5 is a map of the PCM/graphite. the presence of chloride in the card confirms the effectiveness of Infiltration. This map shows the PCM / graphite infiltration path. The EDS processing image shows the distribution of the element in the sample. On the right, before infiltration, graphite foam and carbon images of the extend and size of the voids in the foam structure are shown while in. On the left, foam / PCM composite after infiltration is provided. In the beginning the magnification of EDS picture (Base case) is higher which provides a better picture of the homogeneous infiltration and also its effectiveness for smaller pores. Also, The EDS image and maps verified the presence of the molten chloride salt in the carbon foam. chloride distribution is an indication of the effectiveness of infiltration.

Table 2 shows Solid-phase extraction is an extractive technique which used for solid phase extraction for the Sample Treatments Based on aqueous solvent. The calculated infiltration efficiency is approximately 96% for the first sample. The mass of the substance before soaking in M_d and the mass of the substance after soaking in M_w are shown.

Table 2.
Solid phased Separation sample with one soaking results

	M_d (g)	M_w (g)	Mass changes (g)
Unfiltered	6.46	10.99	ΔW_{ini}= 4.53
Infiltrated	24.84	25	ΔW_{inf}= 0.16

Table 3 reports the soaking measurements for sample two with fluid step extraction. The calculated infiltration efficiency of sample two is approximately 92%. Considering the measured performance, infiltration technique, and process, it was very efficient with an infiltration efficiency of over 90%. Increased efficiency of infiltration improves existing techniques which can be used for a number of

graphite surfaces requiring PCM infiltration. The initial PCM weighed 850 g in the experiment. Four samples were put in the infiltration plan. After removal and cleanup, the mean weight gain of each of the samples was around 18 grams, and therefore for four samples, the overall weight gain was around 72 grams. According to the PCM configuration, only 8.5% of the sample weight was used for infiltration. This significantly decreases proportion of samples compared to the weight of the PCM, which could improve the size of the sample.

Table 3. Liquid extraction process of the soaking sample II

	M_d (g)	M_w (g)	Mass changes (g)
Unfiltered	6.61	11.17	ΔW_{ini}=4.56
Infiltrated	23.66	24.03	ΔW_{inf}=0.37

The solid phase separation sample with soaking results showed that the mass of the substance before soaking was 6.46g, and the mass of the substance after soaking was 24.84g. If the overall weight of the infiltrated PCM at ambient temperature is 18.36 g, based on the density of the material, the amount of the infiltrated substance was measured in relation to the weight of $22.9 \times 10^{-6}\ m^3$.When the porosity of the graphite layer is 70%, the sample diameter is 25 mm, and the height is 50mm, the sample volume is equal to $11.7 \times 10^{-6}\ m^3$. Infiltration efficiency is defined as the ratio of the weight of the final infiltrated sample to the weight of the sample considering that all the pores are being filled with PCM. The infiltration efficiency is estimated to be $\frac{10.9\times10^{-6}\ m^3}{11.7\times10^{-6}\ m^3} \times 100 \approx 93.1\%$. The findings confirm the results of the experiments. infiltration efficiency represents the effectiveness of the infusion process in filling all available voids in graphite foam with PCM. The measured infiltration efficiency of each sample agrees well with the estimated efficiency presented above; validating our efficiency measurements.

PCM-Ca Thermal conductivity was conducted simultaneously by Differential Scanning Calorimetry (DSC) and Netzsch laser flash in three temperature ranges. Figure 6 displays the conductivity values for chloride salt. To offer a more splendid viewpoint on the changes to chloride salts' heat conductivity by graphite foam infiltration, the manufacturer contrasts composite graphite with properties of the PCM conductivity, pure PCM materials and graphite foams.

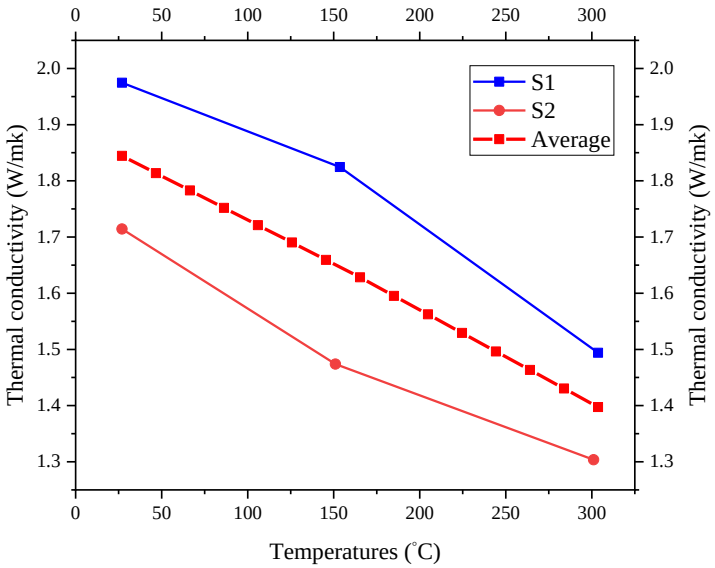

Figure 6. Thermal conductivity for chloride salt pure PCM.

The thermal conductivity of PCM graphite foam calculated in three temperature ranges and related to an increase in the melting point of PCM. Room temperature (23 Celsius degree), 150 Celsius degrees, and 300 Celsius degrees, below the PCM melting point. Triple sampling from various areas of the penetrated foam cylinders was performed. From the food sector to the thermal energy industry and many more, salts of chloride appear to be employed in a broad range of forms. The thermal conductivity range of 1-2 $^{W}/_{m.K}$ chloride salts is usually reported. The thermal conductivity ranges at the lowest values at the maximum temperature range of 50-110 $^{W}/_{m.K}$, as defined in figure 7. Compared to pure chlorides, the thermal conductivity of the chloride and graphite composite is considerably improved. As shown in Figure 7, the thermal conductivity range of pure foam is shown in green. This range has remained constant with temperature changes. While the samples have higher thermal conductivity at low temperatures and with increasing temperature, the average thermal conductivity followed by the melting point of PCM's decreases.

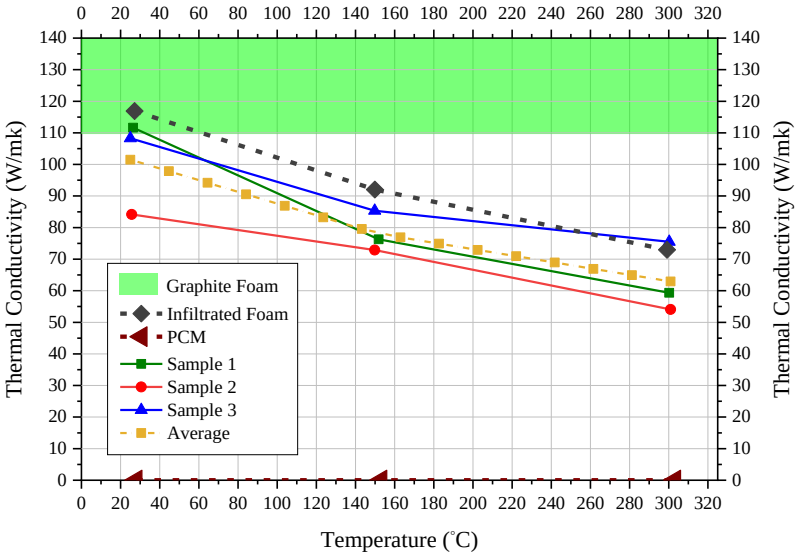

Figure 7. Thermal conductivity of system components. (Samples, Sample Average, Graphite Foam, Pure PCM, Infiltrated Foam).

Thermal conductivity, as the most critical parameter affecting the heat transfer of nanofluids and PCMs, was measured in a temperature range for each sample in the solid phase. Each sample will behave differently in thermal conductivity with temperature changes. Considering the Sample Average, a direct relationship between Graphite Foam infiltrated in the samples and increasing the thermal conductivity is established in this experiment. At lower temperatures (sample at 23 ° C), more negligible effect and at 150 ° C visible and at 300 ° C with latent heat storage melting using phase change materials, higher storage density and minor temperature change Has caused.

Figure 8 shows the measures of thermal conductivity at selected temperatures. Thermal conductivity characterization of composite in contrast to pure PCM is around 45 times greater. This upgrade will improve the technological and economic capabilities of Graphite Foam materials manufacturing reduce carbon dioxide emissions. While the PCM used displays temperature-limited effects of 355 degrees, the process has far-reaching effects and may be used with other PCMs hindered by corrosion. Increasing the thermal conductivity and decreasing the melting temperature of PCMs reduces costs and increases safety. Since the graphite and PCM thermal capacities (ρC_P) in the solid-state is almost the same, thermal diffusiveness improvements ($\alpha = \frac{k}{\rho C_p}$) leads to changes in conductivity and impact on energy storage and charge and discharge speeds. The infiltration is strongly homogeneous, as seen in Figure 4. Thus the spatial variance in thermal conductance is assumed to be small.

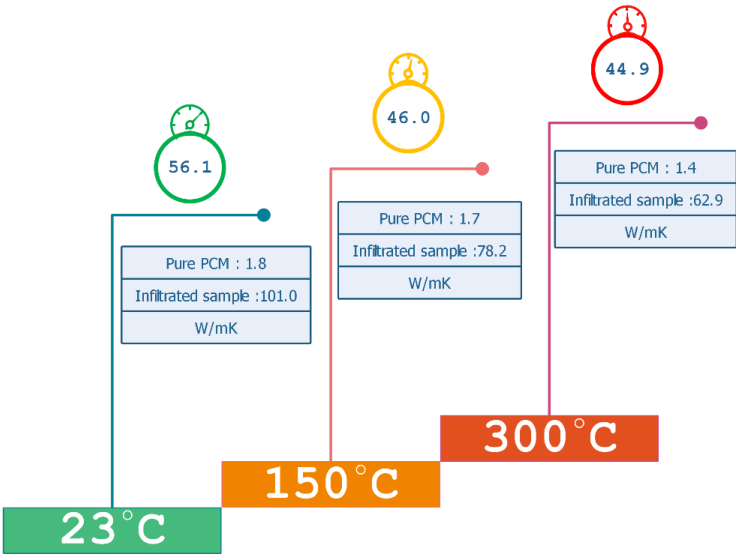

Figure 8. Ratio of Thermal conductivity at different temperatures

To develop high-performance NANO-scale energy storage devices and to design energy storage systems and materials, it is essential to note the properties of thermal stability of recoverable energy storage density. PCM's infiltrated increases the system's thermal conductivity; the graphite decreases PCM volume. energy density (L) is calculated by Equation 9.

$$L = \left[\{\rho \times (1 - \eta_{infil})\} + \{(1 - \rho)\}\right] \times 100 \qquad (9)$$

Where, $1 - \rho$ is equal to the percentage of volume filled by graphite and $1 - \eta_{infil}$ is an amount that filled with cavities instead of salt. The percentage of energy quality loss is calculated at 30.05%. In the solid form, graphite and chloride's heat potential is approximately the same and is not considered in energy density equations. The thermal capacity of graphite is 15% higher than the melting point of PCM composite. This feature can compensate for part of the latent heat storage loss. if this capacity is not used, then the heat storage loss may increase by up to 30%. In general, energy storage increases with increasing thermal conductivity, followed by increased thermal infiltration and energy transfer capacity in a faster time. The infiltrated PCM is expected and needs to stay in the pores of the graphite foam by surface tension forces but could be pushed out of the pores by expansion. The infiltrated sample was analyzed here through a few cycles through which the graphite infiltrated PCM was heated and cooled in thermal and cyclic stability. During the cycle the weight changes of the infiltrated sample were measured for thermal stability calculations. Since spinning, the mass reduction in the samples was far below 18% after many cycles. Further analysis should be carried out to enhance the graphite chloride PCM's capacity to cycle for Outdoor and longer time applications.

Energy storage systems are especially useful in cases of cyclical loading, which allow for alternate absorption/rejection cycles. The number of infiltration cycles is significantly related to the losses and with decreasing cycles, the infiltration mass has decreased. Rarely in some observations did the capsules

have any influence on the PCM. Graphite is used in encapsulated form to prevent possible problems caused by several stages of the heat cycle. In comparison, the proportions of the penetrated graphite are more generous in large-scale systems, with fewer surface area and less PCM leakage from graphite pores. Some high temperature nickel and stainless steel alloys are used in the development of encapsulated graphite infiltrated PCM (EGIPCM) products. EGIPCM may indeed be part of a heat transfer device that could retain and discharge energy at high temperatures into a heat transfer fluid like Supercritical carbon dioxide (sCO_2). Storage of electricity and Heat transfer structures for using graphite infiltrated must be built Efficient EGIPCMs.

4. Conclusions

This study used HTC CFOAM35 NANO-composite with more than 70% porosity for the infiltration project. The filtration pressure has an essential influence on the infiltration effect and the effectiveness therefore vacuum and pressure-assisted infiltration technique have been developed and SEM method was used to analyze the process. Also for infiltration processing, infiltration efficiency test, PCM to raw material infiltration ratio evaluation, energy scattered X-ray spectroscopy (EDS) and image processing were used. Samples of graphite foam are cut to the appropriate shapes and proportions, cylindrical with water jets. Using PCM-equipped capsules, sufficient porosity is injected into the pores of the surfaces and PCM can be maintained. Four samples were placed in the configuration for infiltration. pore diameters ranged from 180 to 984 µm. The rendered images demonstrate that the infiltration device and the vacuum and pressurization process developed in this work effectively achieve PCM infiltration into the nominal 100 to 200 µm foam pores and efficiency were greater than 90%. The average weight gain of each sample after extraction and cleaning was approximately 18 gr, and therefore the total weight gain for 4 samples was approximately 72 gr. Given the initial PCM available in the configuration, only 8.5% was used for infiltration and the remainder was removed, and the net weight of PCM infiltration was calculated to be 18.38 gr with the density of PCM is taken at the ambient temperature. The volume of the PCM infiltrated was calculated from the sample mass changes/PCM density Equal to 22.9 cubic centimeter. Assuming the graphite foam porosity being 70% and the sample dimension of 25 mm diameter and 50 mm height, the total initial void volume of the sample was 11.7 cubic centimeter and the infiltration efficiency was estimated at ≈ 93%. The percentage of energy density loss is measured at approximately 30.05%. Thermal stability was evaluated by measuring the changes in the weight of the infiltrated sample before and after the cycle. The decrease in the mass of the samples after the cycles was less than 18%.

A comparison of the results of the present study with previous studies is worth noting, although researchers have attempted to develop infiltrated graphite-PCM compounds, but little information has been reported on the use of graphite foams with PCM at high temperatures. Lan H et al. investigated the development of high-temperature PCM compounds for solar thermal applications [14]. Al-Jethelah

et al. demonstrated that the use of graphite foams significantly reduces the number of risers required in the storage system[20]. According to Shao et al. The solar thermal conversion efficiency in flexible melamine coated melamine foam phase change material composites is estimated About 90%[8]. Yazici et al. Investigate the resistance limits the system's performance to thermal contact on the surface of the heat exchanger[29]. Qureshi et al. In its up-to-date research, examined graphite foam infiltrated with MgCl as PCM. It turned out that the composite material has significantly higher thermal performance and energy efficiency than LHTES systems[30]. The next phase will require the creation of encapsulations for infiltrated foam PCMs that contribute to EGIPCM being incorporated in a large-scale, effective, and simple energy storage device. The findings encourage activities in this area and increase the production capacity of infiltrated graphite PCM composites for heat storage and other applications at high temperatures.

References

[1] Opolot M, Zhao C, Liu M, Mancin S, Bruno F, Hooman K. Influence of cascaded graphite foams on thermal performance of high temperature phase change material storage systems. Appl Therm Eng 2020;180:115618. https://doi.org/10.1016/j.applthermaleng.2020.115618.

[2] Esmaeili MS, Najafi G. Energy-Economic Optimization of Thin Layer Photovoltaic on Domes and Cylindrical Towers. Int J Smart Grid - IjSmartGrid 2019;3:84–91.

[3] Esameili Shayan M, Najafi G, Esameili shayan S. Design of an Integrated Photovoltaic Site: Case of Isfahan's Jarghouyeh photovoltaic plant. J Energy Plan Policy Res 2021;6:229–50.

[4] Esmaeili Shayan M, Ghasemzadeh F. Nuclear Power Plant or Solar Power Plant. In: Awwad N, editor. Nucl. Power Plants - Process. from Cradle to the Grave, Landon: IntechOpen; 2020. https://doi.org/10.5772/intechopen.92547.

[5] Esmaeili Shayan M. Solar Energy and Its Purpose in Net-Zero Energy Building. In: Pérez-Fargallo A, Oropeza-Perez I, editors. Zero-energy Build. New approaches Technol., IntechOpen; 2020. https://doi.org/10.5772/intechopen.93500.

[6] Ghasemzadeh F, Esmaeili Shayan M. Nanotechnology in the Service of Solar Energy Systems. Nanotechnol. Environ., London: IntechOpen; 2020. https://doi.org/10.5772/intechopen.93014.

[7] Azadbakht M, Esmaeilzadeh E, Esmaeili-Shayan M. Energy consumption during impact cutting of canola stalk as a function of moisture content and cutting height. J Saudi Soc Agric Sci 2015;14:147–52. https://doi.org/10.1016/j.jssas.2013.10.002.

[8] Shao Y wen, Hu W wen, Gao M hang, Xiao Y yuan, Huang T, Zhang N, et al. Flexible MXene-coated melamine foam based phase change material composites for integrated solar-thermal energy conversion/storage, shape memory and thermal therapy functions. Compos Part A Appl Sci Manuf 2021;143:106291. https://doi.org/10.1016/J.COMPOSITESA.2021.106291.

[9] Ghahremannezhad A, Xu H, Salimpour MR, Wang P, Vafai K. Thermal performance analysis of phase change materials (PCMs) embedded in gradient porous metal foams. Appl Therm Eng 2020;179:115731. https://doi.org/10.1016/J.APPLTHERMALENG.2020.115731.

[10] Wang S, Xing Y, Hao Z, Yin J, Hou X, Wang Z. Experimental study on the thermal performance of PCMs based heat sink using higher alcohol/graphite foam. Appl Therm Eng 2021;198:117452. https://doi.org/10.1016/J.APPLTHERMALENG.2021.117452.

[11] Liu H, Fu R, Su X, Wu B, Wang H, Xu Y, et al. MXene confined in shape-stabilized phase

change material combining enhanced electromagnetic interference shielding and thermal management capability. Compos Sci Technol 2021;210:108835. https://doi.org/10.1016/J.COMPSCITECH.2021.108835.

[12] Hajjar A, Jamesahar E, Shirivand H, Ghalambaz M, Babaei Mahani R. Transient phase change heat transfer in a metal foam-phase change material heatsink subject to a pulse heat flux. J Energy Storage 2020;31:101701. https://doi.org/10.1016/j.est.2020.101701.

[13] Karthik M, Faik A, D'Aguanno B. Graphite foam as interpenetrating matrices for phase change paraffin wax: A candidate composite for low temperature thermal energy storage. Sol Energy Mater Sol Cells 2017;172:324–34. https://doi.org/10.1016/j.solmat.2017.08.004.

[14] Lan H, Dutta S, Vahedi N, Neti S, Romero CE, Oztekin A, et al. Graphite foam infiltration with mixed chloride salts as PCM for high-temperature latent heat storage applications. Sol Energy 2020;209:505–14. https://doi.org/10.1016/j.solener.2020.09.029.

[15] Yin Z, Zhang S, Koh S, Linga P. Estimation of the thermal conductivity of a heterogeneous CH4-hydrate bearing sample based on particle swarm optimization. Appl Energy 2020;271:115229. https://doi.org/10.1016/j.apenergy.2020.115229.

[16] El Idi MM, Karkri M. Heating and cooling conditions effects on the kinetic of phase change of PCM embedded in metal foam. Case Stud Therm Eng 2020;21:100716. https://doi.org/10.1016/j.csite.2020.100716.

[17] Badenhorst H. A review of the application of carbon materials in solar thermal energy storage. Sol Energy 2019;192:35–68. https://doi.org/10.1016/j.solener.2018.01.062.

[18] Mitran RA, Lincu D, Buhălțeanu L, Berger D, Matei C. Shape-stabilized phase change materials using molten NaNO3 – KNO3 eutectic and mesoporous silica matrices. Sol Energy Mater Sol Cells 2020;215:110644. https://doi.org/10.1016/j.solmat.2020.110644.

[19] Cheneler D, Kennedy AR. A comparison of the manufacture and mechanical performance of porous aluminium and aluminium syntactic foams made by vacuum-assisted casting. Mater Sci Eng A 2020;789:139528. https://doi.org/10.1016/j.msea.2020.139528.

[20] Al-Jethelah M, Ebadi S, Venkateshwar K, Tasnim SH, Mahmud S, Dutta A. Charging nanoparticle enhanced bio-based PCM in open cell metallic foams: An experimental investigation. Appl Therm Eng 2019;148:1029–42. https://doi.org/10.1016/j.applthermaleng.2018.11.121.

[21] Jana P, Palomo del Barrio E, Dubois M, Duquesne M, Godin A, Vautrin-Ul C, et al. Hydrophobised carbon foams for improved long-term seasonal solar thermal energy storage. Sol Energy Mater Sol Cells 2021;220:110849. https://doi.org/10.1016/j.solmat.2020.110849.

[22] Esmaeili shayan M, Najafi G, Banakar A ahmad. Power Quality in Flexible Photovoltaic System on Curved Surfaces. J Energy Plan Policy Res 2017;3:105–36.

[23] Canseco V, Anguy Y, Roa JJ, Palomo E. Structural and mechanical characterization of graphite foam/phase change material composites. Carbon N Y 2014;74:266–81. https://doi.org/10.1016/j.carbon.2014.03.031.

[24] Singh D, Yu W, Zhao W, Kim T, France DM, Smith RK. Development and prototype testing of MgCl2/graphite foam latent heat thermal energy storage system. Sol Energy 2018;159:270–82. https://doi.org/10.1016/j.solener.2017.10.084.

[25] Rajak DK, Pagar DD, Kumar R, Pruncu CI. Recent progress of reinforcement materials: A comprehensive overview of composite materials. J Mater Res Technol 2019;8:6354–74. https://doi.org/10.1016/j.jmrt.2019.09.068.

[26] Jiang F, Zhang L, She X, Li C, Cang D, Liu X, et al. Skeleton materials for shape-stabilization

of high temperature salts based phase change materials: A critical review. Renew Sustain Energy Rev 2020;119:109539. https://doi.org/10.1016/j.rser.2019.109539.

[27] Lin Y, Alva G, Fang G. Review on thermal performances and applications of thermal energy storage systems with inorganic phase change materials. Energy 2018;165:685–708. https://doi.org/10.1016/j.energy.2018.09.128.

[28] Esmaeili Shayan M, Esmaeili Shayan S, Nazari A. Possibility of supplying energy to border villages by solar energy sources. Energy Equip Syst 2021;9:279–89. https://doi.org/10.22059/EES.2021.246079.

[29] Yazici MY, Saglam M, Aydin O, Avci M. Thermal energy storage performance of PCM/graphite matrix composite in a tube-in-shell geometry. Therm Sci Eng Prog 2021;23:100915. https://doi.org/10.1016/J.TSEP.2021.100915.

[30] Qureshi ZA, Al-Omari SAB, Elnajjar E, Al-Ketan O, Al-Rub RA. Using triply periodic minimal surfaces (TPMS)-based metal foams structures as skeleton for metal-foam-PCM composites for thermal energy storage and energy management applications. Int Commun Heat Mass Transf 2021;124:105265. https://doi.org/10.1016/J.ICHEATMASSTRANSFER.2021.105265.

[31] Li WQ, Zhang TY, Li BB, Cui FQ, Liu LL. Experimental investigation on combined thermal energy storage and thermoelectric system by using foam/PCM composite. Energy Convers Manag 2021;243:114429. https://doi.org/10.1016/J.ENCONMAN.2021.114429.